RHEOLOGICAL CHARACTERIZATION OF A MODEL FOOD SUSPENSION CONTAINING DISCS USING THREE DIFFERENT GEOMETRIES

L.P. MARTÍNEZ-PADILLA[1], L. CORNEJO-ROMERO, C.M. CRUZ-CRUZ and C.C. JÁQUEZ-HUACUJA

Laboratorio de Propiedades Reológicas y Funcionales en Alimentos
Universidad Nacional Autónoma de México
FES-Cuautitlán

AND

G.V. BARBOSA-CÁNOVAS

Biological Systems Engineering Department
Washington State University

Accepted for Publication December 17, 1998

ABSTRACT

The objective of this study was to characterize the flow behavior of a solid-liquid food model which imitates Mexican sauces. The model food suspension consisted of seeds suspended in a shear-thinning fluid (Avicel and Xanthan gum). The effects of size and particle concentration were investigated using a traditional disc geometry in wide gap (spindle), and a ribbon adapted to a rotational viscometer. The effect of particle size was evaluated in a tube viscometer. Power-law parameters and apparent viscosity were estimated in the shear range of each viscometer. The experimental apparent viscosity showed good agreement with predictions obtained using a theoretical expression of relative viscosity for uniform spheres. In all the viscometers investigated, shear-thinning behavior of the suspension was observed, as the aqueous phase, due to low interactions among particles. The ribbon geometry appears to be the best option for flow characterization of food suspensions containing coarse disc shaped particles.

[1] To whom correspondence should be addressed: UNAM FES-Cuautitlán, Departamento de Ingeniería y Tecnología, Av. Primero de mayo s.n., 54740 Cuautitlán Izcalli, Edo de México, México. e-mail: lpmp@servidor.unam.mx

Journal of Food Process Engineering **22** (1999) 55-79.

INTRODUCTION

Many industrial food processes involve the flow of solid-fluid mixtures, in which the knowledge of flow properties is essential for calculations of pumping requirements, heat transfer and mixing operations. Considerable work has been conducted to develop methods of rheological characterization of foods containing suspended material in fluid media, where the suspended solids ($d_p < 4 \times 10^{-4}$ m) are relatively immobile and particle settling is not observed. These products are often considered to be dispersion of solids in fluid media (Rao 1987).

In the food industry, a large number of commercial products which are pumped through pipes contains large size particles (1×10^{-3} m) in Newtonian or non-Newtonian aqueous phase. Examples of solid-fluid mixtures are: blueberry and peach fruit preserves, Mexican sauces, mustards with seeds, and concentrated cream soups, containing between 2-40% w/w of solids. In pumping processes, such mixtures will generally exhibit viscous laminar flow due their relatively high apparent viscosity (>0.10 Pa.s). Nevertheless, few studies have attempted the flow characterization of the whole coarse suspensions. Furthermore, no agreement about the proper methodology to be used has been achieved.

Conventional rheometers which provide a well-defined field in shear flow such as the narrow-gap concentric cylinders or the small angle cone-plate and plate-plate geometries cannot be used due to the small gap required. Some efforts have been made to characterize coarse suspensions with large gap separation. A small shear rate range ($< 10\ s^{-1}$) was obtained using cone-plate geometry (Cross and Kaye 1986) or plate-plate geometry (Pordesimo *et al.* 1994a). However, different ranges of shear rates are found in pumping, heat transfer and mixing operations.

Viscometers with rotating disc or bob in wide gaps can be used for characterization of coarse solid-liquid mixtures where higher shear rate might be obtained. The tube viscometer is another option (Bhamadipati and Singh 1990), but large quantities of test material are needed. However, when a wide diameter or gap size is used, the fluid velocity varies from a maximum value to zero at the wall frontier and some problems can be presented as nonhomogeneous fields caused by slippage at the wall or particle migration in tube and cylinder viscometers (Barnes *et al.* 1989). In the case of a disc immersed in an infinite medium such a spindle, heterogeneous mixing might be observed. Moreover, the constitutive equations for these viscometers from the fundamental rheological variables (shear rate and shear stress) cannot be readily solved. Therefore, in some of the geometries proposed, only an approximation of the shear rate may be obtained, which is dependent upon the flow behavior of the suspension tested (Skelland 1967; Mitschka 1982). Furthermore, not all the

solutions to obtain approximate shear rates are reported for the rheological models, as noted in this literature review.

The use of mixers and mixing principles to evaluate the rheological properties fluids was proposed by Metzner and Otto (1957). Many impellers such as turbines, paddles, anchors, screws, stars, flags, vanes and ribbons have been tested to evaluate the rheological properties of complex food fluids, as reviewed by Castell-Pérez and Steffe (1992), and fermentation broths (Kemblowsky and Kristiansen 1986; Allen and Robinson 1990). Nevertheless, some impellers in viscous flow, such as in mixed stirred tanks or rotating discs, showed only homogeneous mixing around the impeller, slow circulation flow and no fluid motion near the container walls.

The use of helical ribbon, which has numerous industrial applications for the mixing of non-Newtonian fluids, is an alternative way to improve the mixing performance in creeping flow (Tatterson 1991). Allen and Robinson (1990) proved that the helical ribbon was useful in the characterization of filamentous fermentation broths. They also tested a tube viscometer, where good results were obtained when the tube diameter was superior to 0.0116 m. These two current methods can approximate rheological parameters which might be acceptable for engineering applications. However, they have not been applied to flow characterization of coarse particles in a viscous non-Newtonian fluid.

The purpose of this project was to characterize the flow behavior of a model food suspension containing disc shaped particles; (1) in a disc geometry, (2) using a helical ribbon and (3) employing a large tube viscometer. A comparison of rheological parameters and average shear rates was obtained in each rheometer, proposing alternatives and limiting conditions of each one on rheological evaluation of coarse suspensions. The influence of particle size and concentration was studied for small volume samples. The effect of the size in the tube viscometer was also investigated for large volume samples. Experimental apparent relative viscosities or apparent consistency indexes were compared with their respective values, calculated from theoretical expressions for uniform spheres (Happel 1957; Jarzebeski 1981).

CALCULATION PROCEDURES

Flow Behavior Predictions

Several equations to describe the macroscopic behavior of suspensions as linear or power series relationships between relative viscosity (η_r) and particle volume fraction (ϕ) have been summarized (Bernea and Mizrahi 1973; Jinescu 1974). These expressions include empirical, semiempirical and theoretical approaches. Some authors have proposed equations whose form was not a power series, but included the maximum packing fraction of particles (ϕ_{max}), parameter

obtained when the viscosity is infinite. Nevertheless, there is a lack of agreement between the values reported by various authors, probably due to complex interactions taking place at high concentrations (Jinescu 1974).

Considering that the coarse suspensions have less particles than fine suspensions for the same volume fraction, it might be possible to predict the flow behavior of coarse suspensions using mathematical expressions for semi-diluted or semi-concentrated suspensions, due to the low interactions expected between particles.

Theoretical relationships proposed for the viscosity of suspensions of uniform spheres were used to predict the apparent relative viscosity of the model, considering that discs and spheres have a similar behavior. The latter assumption is based by the fact that the drag coefficients for the spheres and discs falling in a fluid have the same curve for $Re_p < 10$ (Rouse and Howe 1953).

The equations and assumptions of the selected relationships are:

(a) The theoretical equation of Einstein (1906), which predicts the relative viscosity of spherical particles for diluted suspensions $\phi < 0.10$. This equation assumes that the mean interparticle distance is very large, compared to the mean solid-particle size. It is also considers slow movement of the particles, no settling effects and no liquid slip relative to the particle surface.

$$\eta_r = 1 + 2.5\phi \tag{1}$$

(b) The theoretical equation of Happel (1957) which was also developed for spherical particles but for semi-concentrated suspensions ($0.05 < \phi < 0.5$). This equation considers a disturbance due to each sphere confined to a functional envelope surrounding it, similar to the behavior of a stream tube for flow inside ducts. Di Felici *et al.* (1991) proved its application for the prediction of the flow of bimodal particle suspensions. Also, the relationship was used to predict the apparent viscosity of coarse spheres and cubes (1×10^{-3} m) suspended in a shear-thinning fluid (Góngora-Nieto *et al.* 1996).

$$\eta_r = (1 + 5.5\phi)\left[\frac{4\phi^{\frac{7}{3}} + 10 - \left(\frac{84}{11}\right)\phi^{\frac{2}{3}}}{10\left(1 - \phi^{\frac{10}{3}}\right) - 25\phi\left(1 - \phi^{\frac{4}{3}}\right)}\right] \tag{2}$$

To establish the comparison of the non-Newtonian suspensions, the apparent viscosity has been evaluated by the ratio of shear stress to shear rate as a function of shear rate in all of the geometries used. The relative viscosity was evaluated at the same shear rate as the ratio of apparent viscosity of suspensions to the apparent viscosity of the carrier fluid.

Some mathematical expressions, as equations modified by Jarzebeski (1981), to predict directly the relative consistency index (m_r) were also tested: (a) the equation of Mooney (1951) (Eq. 3) which in its original form introduced the effect of the dynamic interactions of the spherical particles, and (b) the equation of Frankel and Acrivos (1967) (Eq. 4), which is a theoretical relationship for concentrated suspensions of rigid spheres. These equations have been tested recently to predict the flow behavior in coarse suspensions by Pordesimo *et al.* (1994b).

$$m_r = \frac{9}{8}\left[\frac{\left(\frac{\phi}{\phi_{max}}\right)^{1/3}}{1-\left(\frac{\phi}{\phi_{max}}\right)^{1/3}}\right]^n \tag{3}$$

$$\ln(m_r) = \left[\frac{2.5\phi}{1-C\phi}\right]^n \tag{4}$$

Data Evaluation

Disc Geometry. The method proposed by Mitschka (1982) for a power-law fluid was used to evaluate the average shear stress ($\bar{\sigma}$) and the average shear rate ($\bar{\dot{\gamma}}$) by the following expressions:

$$\bar{\sigma} = k_{L\sigma} L_i \tag{5}$$

$$\bar{\dot{\gamma}} = k_{N\dot{\gamma}(n)} N \tag{6}$$

The flow behavior index (n), necessary for those calculations, was obtained by the slope of the logarithmic plot of L_i vs N. The conversion factors $k_{L\sigma}$ (which

is a function of the spindled used), and $k_{N\dot{\gamma}(n)}$ (which is a function of the spindled used and n), were taken from data reported by Mitschka (1982).

Ribbon Geometry. The average shear rate ($\bar{\dot{\gamma}}$) was calculated by the Metzner and Otto (1957) relationship as:

$$\bar{\dot{\gamma}} = k_{\dot{\gamma}} N \tag{7}$$

where the constant of proportionality $k_{\dot{\gamma}}$ was evaluated by Eq. 8 (Brito *et al.* 1992). This equation is based on the papers of Bourne and Buttler (1969) and Ulbrecht and Carreau (1985), where the flow between the rotating helical surface and the vessel wall was simulated by a Couette flow. A ratio of vessel diameter to the ribbon diameter close to 1.1 was appropriate to approximate the system to a narrow-gap concentric cylinder. The expression obtained (Eq. 8) was based only on the ribbon geometry and n, which was also evaluated as the slope of the logarithmic plot of M vs N:

$$k_{\dot{\gamma}} = \frac{4\pi\left[\left(\frac{D_v}{d_e}\right)^2 - 1\right]^{\frac{1}{n-1}}}{\left[n\left(\frac{D_v}{d_e}\right)^{\frac{2}{n}} - 1\right]^{\frac{n}{n-1}}} \tag{8}$$

In Eq. (8), d_e = 0.0617 m, is the equivalent inside diameter of the ribbon used, obtained as proposed by Chavan and Ulbrecht (1973), and D_v is the vessel diameter. For the calculation of the average shear stress ($\bar{\sigma}$) the following relationship proposed by Kemblowsky and Kristiansen (1986) was used:

$$\bar{\sigma} = \frac{2\pi M k_{\dot{\gamma}}}{k_p d_i^3} \tag{9}$$

The geometric constant k_p = 276.16, required for the average shear stress calculation, was evaluated from the classical dimensionless Power-number (N_p)

vs impeller Reynolds number (Re_m) correlation (Eq. 10). Viscosity standards of 0.092, 0.477 and 0.976 Pa.s (Brookfield Eng. Lab. Inc., MA) were used to obtain k_p in a Re_m range from 0.01 to 10. A difference of less than 1% exists between the experimental and the predicted k_p value by the relationship proposed by Chavan and Ulbrecht (1973).

$$N_p = \frac{k_p}{Re_m} \tag{10}$$

Tube Geometry. Shear stress at the wall (σ_w) and shear rate at the wall ($\dot{\gamma}_w$) were calculated using results of pressure drop (ΔP) and average suspension velocity ($\bar{V}_s$) with the classical Rabinowitsch-Mooney relationships for the power-law fluids for each velocity.

This method is based in the following assumptions: (a) The flow occurs in a horizontal tube and is isothermal, steady and laminar, (b) The fluid is incompressible and time-independent power-law, (c) There is no slippage at the wall, (d) There is no radial or tangential components of the fluid velocity, (e) The kinetic energy is constant (Skelland 1967; Govier and Aziz 1972). To follow these assumptions, long, straight pipe sections are necessary before and after pressure drop sensors (steady velocity distribution). The minimal entrance length (Le) for laminar flow of Newtonian fluids through pipes was calculated by the following expression (Bird *et al.* 1977):

$$Le/D = 0.035\ Re \tag{11}$$

An approximation for a power law fluid was obtained using the same expression and introducing a generalized Reynolds number (Re_{gen}).

The equation to calculate the shear stress at the wall (σ_w) was:

$$\sigma_w = \frac{D\Delta P}{4L} \tag{12}$$

The expression for the shear rate at the wall ($\dot{\gamma}_w$) was:

$$\dot{\gamma}_w = \frac{8\overline{V}_s}{D}\left[\frac{3n+1}{4n}\right] \tag{13}$$

And n was calculated as:

$$n = \frac{d\ln\sigma_w}{d\ln\dot{\gamma}_w} \tag{14}$$

MATERIALS AND METHODS

Physical properties of several food suspensions were evaluated. The properties selected to prepare the model food were: fluid and particle density, fluid viscosity, size and particle shape. The suspensions tested were prepared based on the properties of the Mexican commercial sauces, which had a shear-thinning carrier fluid, discs of millimetric size, and similar particle and fluid density.

The liquid phase, a shear-thinning fluid, was prepared by mixing Xanthan gum (Keltrol, Kelco Division of Merck & Co Inc.) and Avicel RC-59, which is a commercial mixture of microcrystalline cellulose with carboxymethil-cellulose (FMC Corporation). For small samples respectively, mixtures of 0.5-0.8%, and for large samples (tube viscometer) mixtures of 0.6-0.8% were used, due to differences obtained from laboratory to pilot plant preparation. These mixtures were chosen in a preliminary test because they avoided particle settling and apparent viscosity was time-independent of shear (shear thinning fluid).

Flow characterization of the aqueous phase was measured in a rotational viscometer (Contraves-Mettler Rheomat 115; Mettler-Toledo A.G., Switzerland) at 25C $\pm$ 0.1 using a temperature control vessel and a temperature bath (Rheotherm RT51, Mettler-Toledo A.G., Switzerland). A Couette geometry was used with conical bottom cylinders (MS DIN 125, according to DIN 53019); bob and cup radius of 0.0248 m and 0.027 m, respectively. A shear rate program of 0.6 to 89.1 to 0.6 s^{-1} was applied during 5 min, to obtain the up-down curves. Flow parameters of the aqueous phase were also obtained in the three geometries proposed for comparison purposes. The density of the continuous phase was measured by picnometry, while the particle densities were determined by liquid displacement techniques (Koichi *et al.* 1991).

Pepper and tomato seeds were the particles chosen as the solid phase, since they have regular geometry and are included in many Mexican type sauces. The effect of diameter was evaluated using seeds of 0.002, 0.004 and 0.005 m.

Concentrations from 5 to 40% w/w of seeds were found in commercial samples of Mexican sauces. Concentrations studied here were 10, 15 and 20% w/w when a small sample was required, and 5% w/w when a tube viscometer was used. Three replicates were prepared for all studies two hours before the test to achieve particle hydration.

Measurement of Flow Behavior Properties Using a Disc Geometry in a Wide Gap (Spindle)

Flow behavior curves were obtained using a Brookfield RVT Viscometer (7.187×10^{-3} Nm) with the spindle set, 8 speeds (Brookfield Eng. Lab. Inc., MA). All the rheological measurements were carried out at 25C±1. The containers were placed into a controller temperature bath (RT 200 Brookfield Eng. Lab. Inc., MA). The rotational speed (N) was changed manually, increasing from 0.5 to 100 rpm and decreasing to 0.5 rpm, during 2 min at each speed, and the percentage torque reading (L_i) was taken. To check the viscometer calibration a viscosity standard of 0.477 Pa.s (Brookfield Eng. Lab. Inc., MA) was used.

Measurement of Flow Behavior Properties with Ribbon Geometry

A helical ribbon impeller (stainless steel) was adapted to a rotational viscometer Rheomat 115A (50×10^{-3} Nm)(Contraves-Mettler, Mettler-Toledo A.G., Switzerland) controlled by a computer. Figure 1 shows the dimensions of the impeller, and the acrylic vessel that was used as a container. The rheological measurements were carried out at 25C ± 1 (the container was placed into a controller temperature bath, Rheotherm RT51, Mettler-Toledo A.G., Switzerland). This technique is based on the determination of the torque (M) of the impeller as a function of N, and calculate the average shear stress ($\bar{\sigma}$) and the average shear rate ($\bar{\dot{\gamma}}$). The proportionally constants k_σ and $k_{\dot{\gamma}}$ were introduced as input data in the software used (SWR37 Mettler-Toledo A.G., Switzerland). The shear rate was programmed, 0.48-78-0.48 s^{-1}, during 5 min and the respective values were registered and stored. This range was fixed as a function of maximum torque reading.

Measurement of Flow Behavior Properties with Tube Viscometer

A pilot plant flow system with a progressive cavity positive displacement pump (Sine pump model SPS-20, Div Kontro Co., Orange, MA) was used. A stainless steel pipe (0.035 m internal diameter), was assembled as a tube viscometer (Fig. 2). The velocity was changed from 0.02 to 0.5 m/s and from 0.5 to 0.02m/s using an electronic frequency driven speed control. The suspension flow was measured using a test tube (0.002 m^3) and a stopwatch

(0.01s accuracy). The flow system was equipped with two transparent tubes to facilitate the recording of the suspension motion. The suspensions (0.045 m^3) were pumped at different flow rates at room temperature (25 ± 1C) and atmospheric pressure (548 mm Hg). The measurement points were located 2.1 m after a sudden contraction (Le/D = 60) and 4.5 m (Le/D = 128) before a 90° elbow. The pressure drop of 4.5 m of horizontal tube (L/D = 128) was measured with two U-tube open manometers. The flow was maintained as laminar ($2 < Re_{gen} < 20$), and for each suspension ten different flow rates were tested with three replicates.

D_v/d_i	w/d_i	s/d_i	l/d_i	H/d_i
1.1	0.15	0.5	0.99	1.29

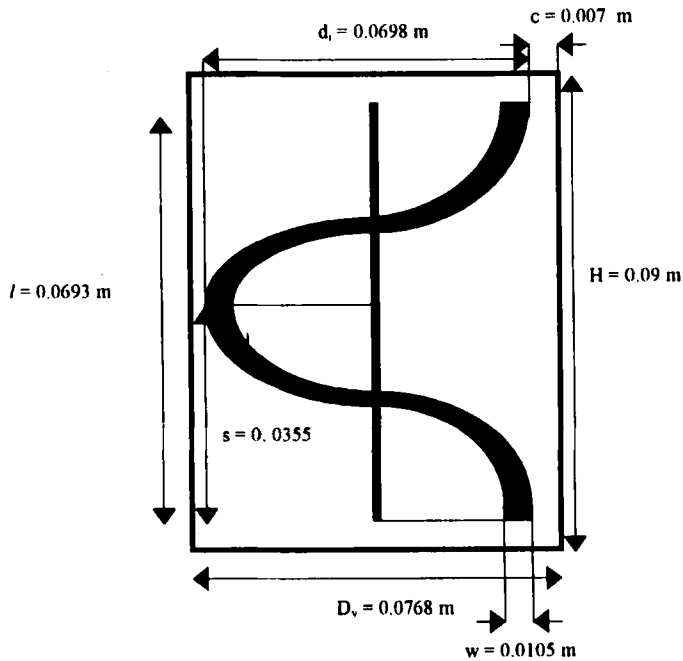

FIG. 1. PRINCIPAL DIMENSIONS OF ACRYLIC VESSEL AND HELICAL RIBBON IMPELLER

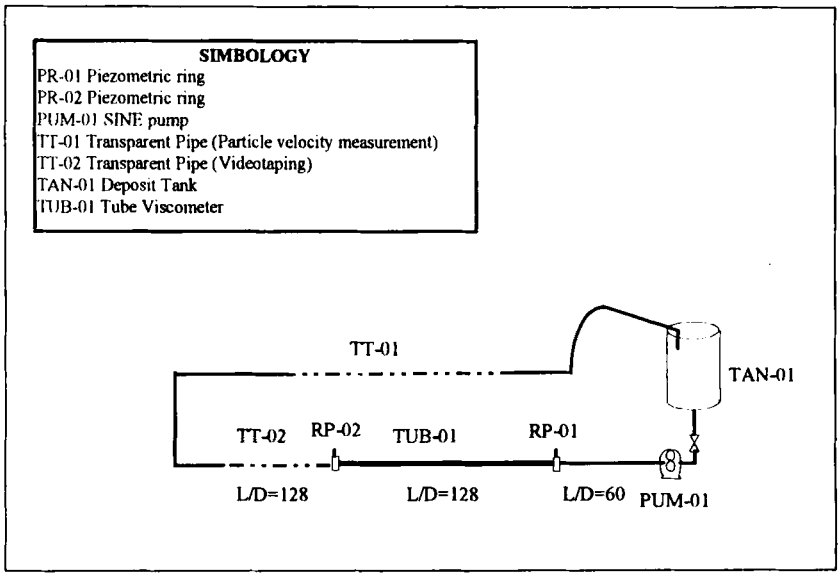

FIG. 2. SCHEMATIC DIAGRAM OF THE PILOT PLANT PUMPING SYSTEM

RESULTS

The average density of the whole commercial sauces was 1046 ± 6.9 kg/m^3, while the aqueous phase density was 1039 ± 5.1 kg/m^3. Seeds density found in commercial sauces varied from 900 to 1100 kg/m^3. These properties were used to select the characteristics of the proposed model. Fluid density of the model food suspension was 996 kg/m^3 for mixtures of Avicel 0.8%-Xanthan gum 0.5%, and 994 kg/m^3 for mixtures of Avicel 0.8%-Xanthan gum 0.6%. Particle densities were 1015, 1030, and 920 kg/m^3, for particles of 0.002, 0.004, and 0.005 m diameter. At rest, no settling was observed due to close densities (particle-fluid), and to the apparent viscosity of the fluid. This apparent viscosity was enough to allow laminar flow and was able to maintain the particles in suspension.

The shear stress, shear rate and apparent viscosity were estimated at each velocity using for calculations the outputs given by each viscometer proposed in this study. Each rheogram includes the mean of three replicates, and their correlation coefficients are reported. The suspensions showed the same non-

Newtonian behavior of the aqueous phase due to the fact that lines are parallel in the well known log-log plot of all of the geometries tested (Fig. 4, 5, 6). This phenomena is probably due to the low interactions between particles. Some authors, as reviewed by Jinescu (1974), reported a change in the rheological behavior from Newtonian to non-Newtonian when the number of particles exceeded a given value of critical concentration. Newtonian behavior may change to shear thinning behavior when the particle concentration is increased, and shear thinnining may change to thixotropic behavior. These flow behaviors have been justified as a result of particle interactions due to the hydrodynamic or an electrostatic nature of the particles.

Flow curves of the non-Newtonian aqueous phase in a Couette, ribbon and disc geometries are shown in Fig. 3. Similar shear stresses and apparent viscosities are observed for the three geometries tested. Small deviations are found at lower shear rates ($< 10\ s^{-1}$). These results confirmed the validity of the proposed methods. The flow curve of the tube viscometer is not included because Xanthan concentration is high (0.6%).

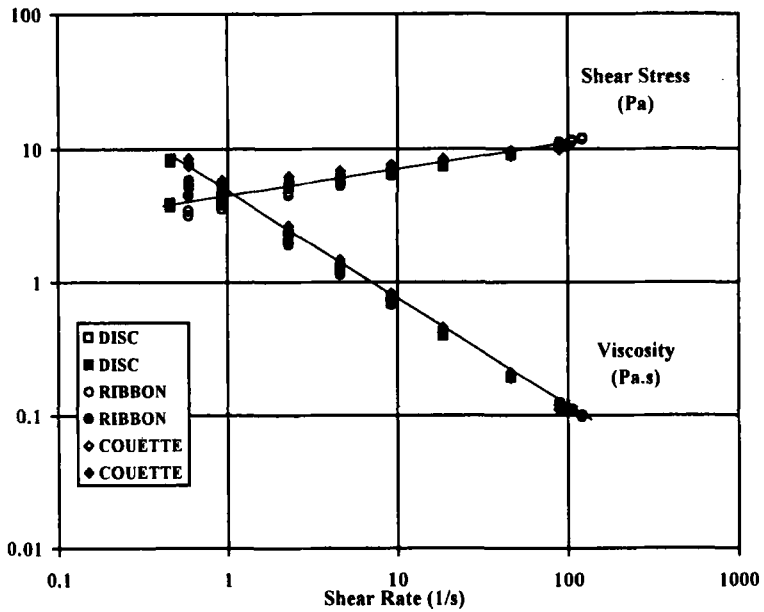

FIG. 3. EXPERIMENTAL FLOW CURVES OF THE AQUEOUS PHASE OBTAINED WITH DISC, RIBBON AND COUETTE GEOMETRIES

Very low shear rates ($< 0.1\ s^{-1}$) were not obtained due to limitations of the pump and instruments used. Therefore, zero viscosity was not achieved. The power-law parameters of the three replicates were calculated in the range of shear rate depending on the suspension tested and geometry used. Tables 2, 3, and 4 show apparent viscosities evaluated at $60\ s^{-1}$ (shear rate chosen arbitrary but comprise in the three geometries ranges), and their respective relative viscosities. For comparison purposes apparent relative viscosities were calculated for the suspensions studied using the theoretical expressions proposed by Einstein (1957) (Eq. 1) and Happel (1957) (Eq. 2). The first one predicts values ranging from 1.25 to 1.5. The second predicts higher values ranging from 1.7 to 3.0, which are close to experimental results obtained.

Comparison of the experimental power law parameters with those from the literature is difficult because no complete data sets are available and particle shape is different. The equations of Mooney (1951) (Eq. 3), and Frankel and Acrivos (1967) (Eq. 4), modified by Jarzebski (1981) were used to estimate power-law consistency indexes. A value of 1.2 was used for C, empirical parameter relating the packing geometry of the dispersed phase. A value of 0.83 for the critical volume fraction was used (Pordesimo *et al.* 1994b). Equation 3 predicted relative consistency indices (m_r) ranging from 1.2 to 1.9 for concentrations of 4.8 to 19.4% (v/v), while Eq. 4 gave lower m_r, ranging from 1.01 to 1.3. Nevertheless, when comparing both predictions with experimental results, the m_r obtained were considerably higher independently of the viscometer used, ranging from 1.18 to 3.8 for the same concentrations.

Flow Behavior Properties Using a Disc Geometry in a Wide Gap (Spindle)

The spindle #3 of the Brookfield RVT viscometer was selected for all the samples studied, since torque readings were between 10 to 90%. Respective values of $k_{L_\sigma} = 0.279$, and interpolated values of $k_{N\dot{\gamma}(n)}$, which varied from 0.92 to 1.08 depending on the n obtained, were taken from Mitschka (1982).

Some irregularities in the flow curves were observed due to particle collisions with the rotating disc. It is important to remark that only the up-curves were used here in the analysis, since a pseudo-homogeneous suspension was achieved only in these curves. For the down-curves the torque readings were increased due to migration of particles near to the rotating spindle. This phenomena was present in all the suspensions tested.

Typical up-curves are plotted in Fig. 4 for a particle diameter of 0.004 m. As expected the suspensions showed higher shear stresses and apparent viscosities than the aqueous fluid. When the apparent viscosity was compared with the curve of the Happel prediction, only the suspension with concentration of 10% w/w and 0.004 m was close. Suspensions of 15 and 20% w/w were

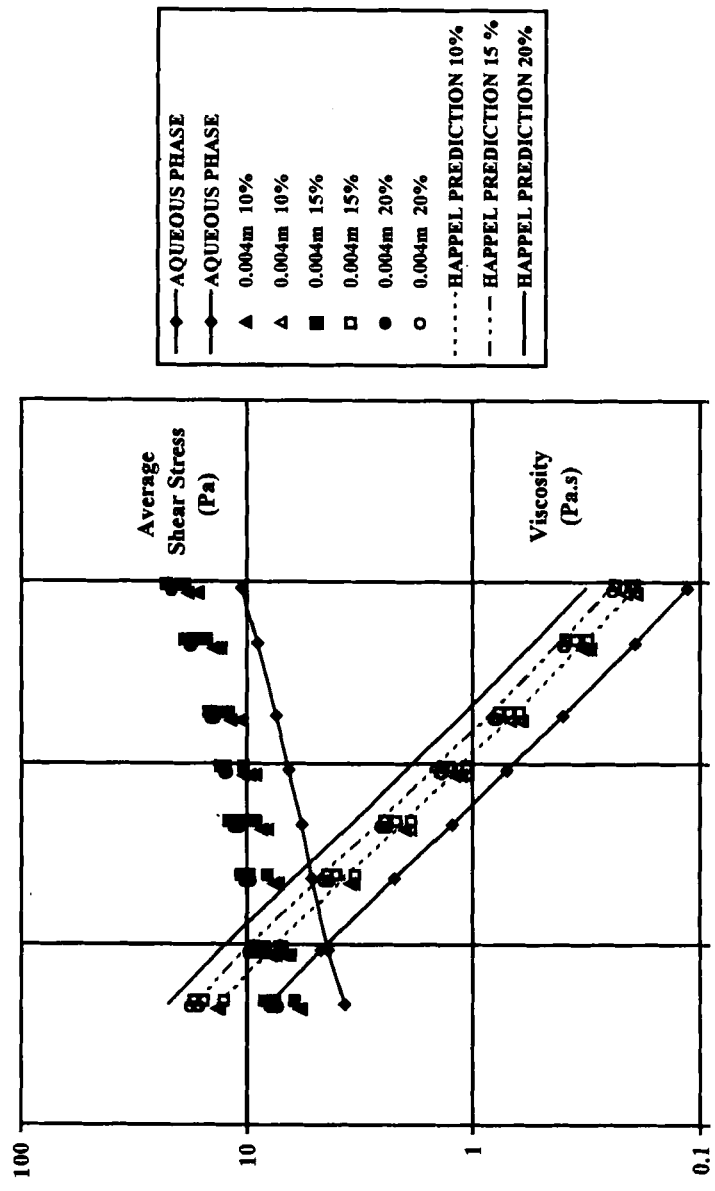

FIG. 4. EXPERIMENTAL FLOW CURVES FOR DIFFERENT CONCENTRATIONS (10%, 15% AND 20%, W/W) OF SUSPENSIONS CONTAINING 0.004 m PARTICLE DIAMETER OBTAINED WITH DISC GEOMETRY
The Happel Prediction and the aqueous phase flow curve are also included.

overlapped, both of them showing more deviation between replicates than suspensions of 10% w/w.

Fluid and suspensions rheological parameters obtained with the disc geometry (spindle) are summarized in Table 1. When the power law parameters of the suspensions and the carrier fluid were compared, a small decrease in the flow behavior index and an increase in the consistency index (m) were found, as a function of the particle concentration. These results followed the same patterns as the inorganic particles in a power-law fluid (Jinescu 1974) or coarse food particles in the same kind of fluid (Pordesimo *et al.* 1990a). Nevertheless, there was no defined tendency of those parameters. At 10% w/w all of the suspensions studied containing different particle sizes showed as expected a similar m (6.3, 6.6 and 6.6 $Pa.s^n$), and also a similar apparent viscosity. This result can be explained by the low concentration where the particles are still suspended (pseudo-homogeneous fluid), and the agitation is not enough to give more interactions between particles, or to favor the particle migration to the rotating disc. However, for more concentrated suspensions, consistency indexes were different, for a concentration of 15% w/w (6.8, 8.0, and 7.5 $Pa.s^n$) or for a concentration of 20% w/w (7.7, 8.5 and 8.4 $Pa.s^n$).

When experimental relative apparent viscosity (η_{exp}) (evaluated at 60 s^{-1}) was compared with the viscosity obtained from Happel's theoretical equation (η_{pred}), there was a high relative error ranging from -6 to -66%. The relative error was calculated as $(\eta_{exp} - \eta_{pred})/ \eta_{exp} \times 100$. Results confirmed that this kind of suspensions are not able to be characterized using this geometry.

Flow Behavior Properties Using Ribbon Geometry

To conduct the proper calculations of the selected ribbon, and average $k_{\dot{\gamma}}$ = 29.05 was used instead of punctual values, considering the small variation of this constant, from 28.64 to 30.47 in the whole range of the flow behavior index (0.1 to 1.0). Using this geometry, irregularities in the up-down curves were also observed. Nevertheless, both of the curves showed similar flow parameters, with better regression coefficients in the down-curves. These results can be attributed to the improved mixing in the up-curve execution, loading to a suspension flow behavior of a pseudo-homogeneous fluid. In the down-curve the flow was stabilized, and the torque readings showed less perturbations.

When comparing the shear stress and the apparent viscosity of suspensions with its respective values in the aqueous fluid (Fig. 5), a bigger separation was observed between the flow curves than in the disc geometry case, evidencing the effect of particle concentration. Suspensions of 0.005 m particle diameter showed the most irregular curves, and sometimes these particles caused obstructions in the close clearance of the impeller. In this geometry the Happel prediction (Eq. 2) is close for 10% w/w and 15% w/w concentrations except for

TABLE 1
AQUEOUS PHASE AND SUSPENSION FLOW PARAMETERS FOR DIFFERENT SUSPENSION PARTICLE DIAMETERS (d_p) AND CONCENTRATIONS (% W/W) OBTAINED WITH A DISC GEOMETRY IN A WIDE GAP (SPINDLE #3)

d_p (m)	% w/w	n	m (Pa.s^n)	# of data points	r	$\bar{\dot{\gamma}}$ (1/s)	Apparent viscosity (Pa.s) @ 60 s^{-1}	Relative viscosity	Happel Predicted relative viscosity	Relative error %
AQUEOUS PHASE		0.19	4.4	24	0.997	0.46-97.5	0.160			
0.002	10	0.19	6.3	24	0.987	0.50-98.8	0.229	1.4	1.7	-19
0.002	15	0.19	6.8	24	0.977	0.46-94.1	0.247	1.5	2.2	-47
0.002	20	0.21	7.7	24	0.950	0.43-88.4	0.303	1.9	2.8	-47
0.004	10	0.20	6.6	24	0.980	0.43-94.1	0.250	1.6	1.7	-6
0.004	15	0.19	8.0	24	0.976	0.47-102.3	0.290	1.8	2.2	-22
0.004	20	0.19	8.5	24	0.993	0.45-97.3	0.308	1.9	2.8	-47
0.005	10	0.18	6.6	24	0.982	0.50-99.4	0.230	1.4	1.8	-22
0.005	15	0.20	7.5	24	0.985	0.42-84.7	0.283	1.8	2.3	-28
0.005	20	0.18	8.4	24	0.976	0.44-89.4	0.292	1.8	3.0	-66

(n) FLOW BEHAVIOR INDEX, (m) CONSISTENCY INDEX, AND (r) CORRELATION COEFFICIENT OF THE LOG-LOG SHEAR STRESS-SHEAR RATE CURVES.

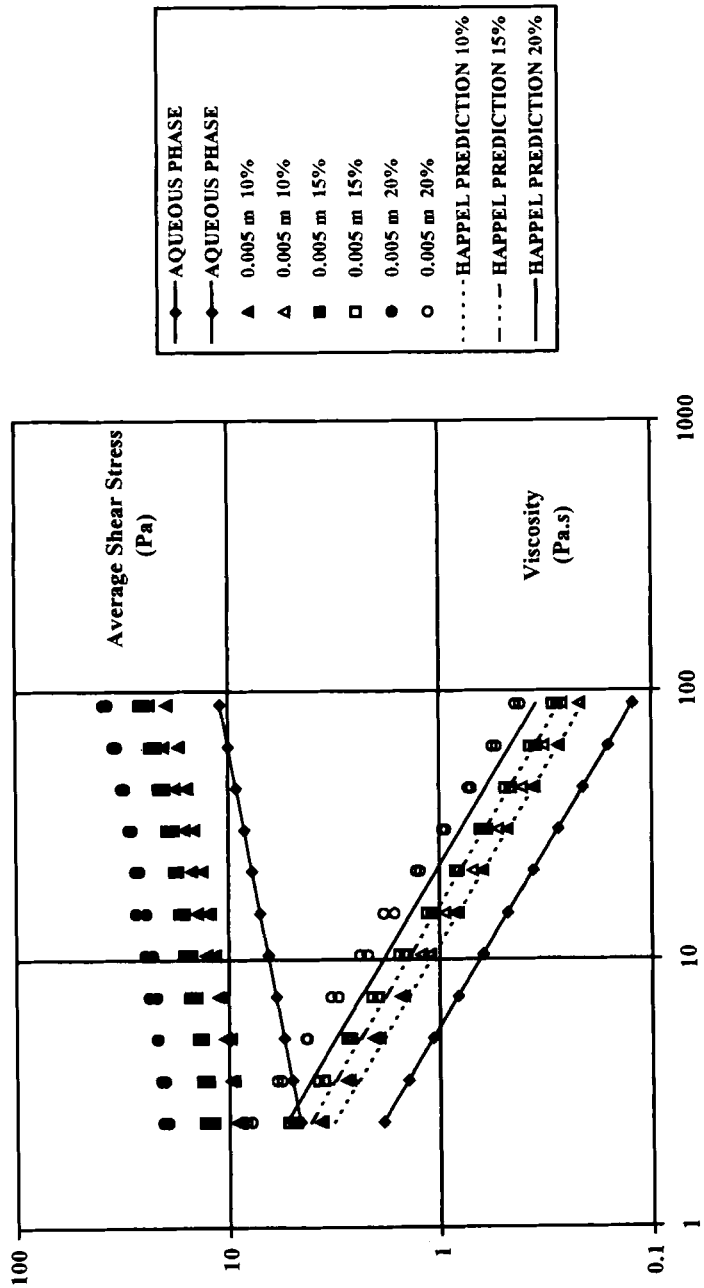

FIG. 5. EXPERIMENTAL FLOW CURVES FOR DIFFERENT CONCENTRATIONS (10%, 15% AND 20%, W/W) OF SUSPENSIONS CONTAINING 0.005 M PARTICLE DIAMETER OBTAINED WITH RIBBON GEOMETRY
The Happel Prediction and the aqueous phase flow curve are also included.

concentrations of 20% w/w where the predictions are lower than the experimental results. Latest result can be explained because gross particles presented more resistance and/or interactions between them, and they are not considered in the Happel equation.

Power law parameters and relative apparent viscosity obtained with ribbon geometry are presented in Table 2. In this geometry, when an increase of particle concentration in 0.004 or 0.005 m suspensions particle diameter was carried out, a linear increase of consistency index (m) was observed. If the concentration is maintained constant (15%) and the particle diameter varied, a similar m is observed for particles of 0.002 and 0.004 m (9.3, 9.4 Pas^n).

A comparison of relative viscosity evaluated at $60s^{-1}$ with predicted viscosity obtained with Happel's equation is shown in Table 2. It was found that in the prediction, the relative error varies from 5 to 21%. The largest deviation (21%) was obtained with concentrations of 20% w/w and 0.005 m particle diameter. Results suggest that 15% w/w is the maximum concentration predicted with Happel's equation for the suspensions studied.

Flow Behavior Properties Using Tube Viscometer

Shear stress at the wall in the tube viscometer as a function of shear rate at the wall is shown in Fig. 6. Critical velocities were not detected in the well known plot log $\Delta p/L$ vs log $\overline{V}_s$, and only straight lines were obtained, indicating that the symmetric flow existed (Govier and Aziz 1972). Videorecorded flows confirmed these results, where no laying bed and nonrotation of particles were detected. In this case the horizontal tube can be taken as a tube viscometer.

Power law parameters calculated for the suspensions at concentration of 5% w/w shows an increase in m compared with the fluid without particles as obtained in the other viscometers with more experimental deviations (Table 3). Nevertheless, the difference in relative viscosity predicted using Einstein equation (Eq. 1) is closer than the Happel prediction (Eq. 2), when compared with the experimental apparent viscosity (less than 7%). These results confirm that the disc-suspensions containing lower than 5% w/w can be considered as diluted suspensions. In this geometry, the investigation of more concentrated suspensions was not possible since sedimentation was observed when flowing at higher particle concentrations.

CONCLUSION

The flow behavior of a model food suspension with discs was characterized as a shear thinning fluid like the carrier fluid. The ribbon geometry seems to better characterize the flow behavior of coarse suspensions containing disc-shaped particles since pseudo-homogeneous flow can be maintained and

TABLE 2
AQUEOUS PHASE AND SUSPENSION FLOW PARAMETERS FOR DIFFERENT SUSPENSION PARTICLE DIAMETERS (d_p) AND CONCENTRATIONS (% W/W) OBTAINED WITH RIBBON GEOMETRY

d_p (m)	% w/w	n	m ($Pa.s^n$)	# of data points	r	$\bar{\dot{\gamma}}$ (1/s)	Apparent viscosity (Pa.s) @ 60 s^{-1}	Relative viscosity	Happel Predicted relative viscosity	Relative error %
AQUEOUS PHASE		0.24	3.7	27	0.99	0.48-72.7	0.165			
0.002	15	0.21	9.3	27	0.99	0.48-72.7	0.366	2.2	2.2	0
0.004	10	0.19	7.3	27	0.99	0.48-72.7	0.265	1.6	1.7	-6
0.004	15	0.19	9.4	27	0.95	0.48-72.7	0.341	2.1	2.2	-5
0.004	20	0.18	14.0	27	0.96	0.48-72.7	0.529	3.2	2.8	12.5
0.005	10	0.24	6.8	27	0.97	0.48-72.7	0.303	1.8	1.8	0
0.005	15	0.27	8.4	27	0.95	0.48-72.7	0.422	2.6	2.3	11.5
0.005	20	0.24	14.0	27	0.95	0.48-72.7	0.623	3.8	3.0	21

(n) FLOW BEHAVIOR INDEX, (m) CONSISTENCY INDEX, AND (r) CORRELATION COEFFICIENT OF THE LOG-LOG SHEAR STRESS-SHEAR RATE CURVES.

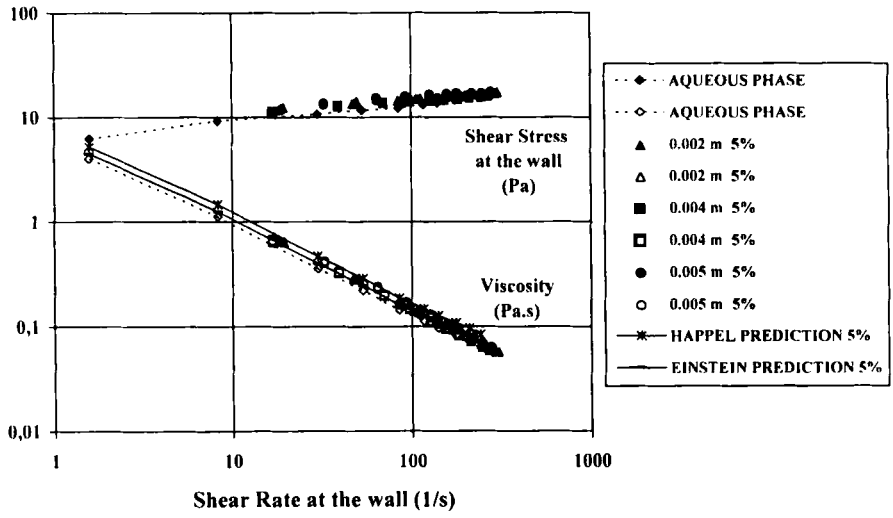

FIG. 6. EXPERIMENTAL FLOW CURVES FOR DIFFERENT SUSPENSION PARTICLE DIAMETERS (0.002 m, 0.004 m, AND 0.005 m) AND A CONCENTRATION OF 5% (W/W) IN THE TUBE VISCOMETER
The Happel and Einstein Prediction, and the aqueous phase flow curve are also included.

comparative small samples are required. Comparisons of experimental results of relative consistency index and relative apparent viscosity with the respective theoretical expression reported in the literature, the Happel (1957) relationship for the viscosity of the suspensions of uniform spheres gives the closer predictions for suspensions studied up to 15% w/w, or the Einstein equation for diluted discs suspensions (>5% w/w). Furthermore, only the volume fraction was needed to make such predictions, that is highly appreciated in pumping calculations. Finally, this study presented an effective and simple methodology to evaluate flow parameters of food suspensions with medium apparent viscosity of the continuous phase (0.1-1.0 Pa.s) and disc shaped particles (1×10^{-3}m). For flow characterization of more concentrated suspensions or higher viscous fluid media a similar helical ribbon geometry with a high torque ($>50 \times 10^{-3}$ Nm) rheometer is recommended.

TABLE 3
AQUEOUS PHASE AND SUSPENSION FLOW PARAMETERS FOR DIFFERENT SUSPENSION PARTICLE DIAMETERS (d_p) AND CONCENTRATIONS (% W/W) OBTAINED WITH TUBE GEOMETRY

d_p (m)	% w/w	n	m (Pa.s^n)	# of data points	r	$\bar{\dot{\gamma}}$ (1/s)	Apparent viscosity (Pa.s) @ 60 s^{-1}	Relative viscosity	Happel Predicted relative viscosity	Relative error %	Einstein Predicted relative viscosity	Relative error %
AQUEOUS PHASE		0.15	6.6	30	0.98	1-240	0.203					
0.002	5	0.12	8.5	30	0.99	19-294	0.232	1.14	1.30	-14	1.12	2
0.004	5	0.13	7.8	26	0.99	17-270	0.221	1.09	1.29	-18	1.12	-3
0.005	5	0.12	9.1	20	0.96	33-280	0.248	1.22	1.33	-9	1.13	7

(n) FLOW BEHAVIOR INDEX, (m) CONSISTENCY INDEX, AND (r) CORRELATION COEFFICIENT OF THE LOG-LOG SHEAR STRESS-SHEAR RATE CURVES.

NOMENCLATURE

C	Empirical constant (Eq. 4)
d_i	Impeller diameter (m)
d_e	Equivalent inside diameter (m)
d_p	Particle diameter (m)
D	Diameter of tube (m)
D_v	Vessel Diameter (m)
$k_{L\sigma}$	Conversion factor (Eq. 5)
$k_{N\dot{\gamma}(n)}$	Conversion factor (Eq. 6)
k_p	Geometric constant (Eq. 10)
$k_{\dot{\gamma}}$	Proportionality constant (Eq.7)
L	Length of tube (m)
L_e	Entrance length (m)
L_i	Percentage torque reading (%)
m	Consistency index ($Pa.s^n$)
m_r	Consistency index ($Pa.s^n$)
M	Torque (N.m)
n	Flow index
N	Rotational speed (1/s)
N_p	Power number
ΔP	Pressure drop (Pa)
R	Tube radius (m)
Re	Reynolds number
Re_{gen}	Generalized Reynolds number for a power law fluid
Re_m	Impeller Reynolds number
Re_p	Particle Reynolds number
$\bar{V}_s$	Average suspension velocity (m/s)
V	Volume (m^3)

Greek Letters

$\bar{\dot{\gamma}}$	Average Shear rate (1/s)
$\dot{\gamma}_w$	Shear rate at the wall (1/s)
ϕ	Volume Fraction ($V_p/(V_p+V_f)$)
ϕ_{max}	Maximum packing fraction of particles
ρ	Density (kg/m^3)
$\bar{\sigma}$	Average Shear stress (Pa)
σ_w	Shear stress at the wall (Pa)

η Apparent shear viscosity (Pa s)
η_r Relative viscosity

ACKNOWLEDGMENTS

This study was supported by a grant obtained from DGAPA-UNAM (Project IN302193). Additional funds were received from the National Council of Science and Technology (CONACYT, México) to partially support Dr. L.P. Martínez-Padilla as Visiting Professor at Washington State University, Pullman WA.

REFERENCES

ALLEN, D.G. and ROBINSON, C.W. 1990. Measurement of rheological properties of filamentous fermentation broths. Chem. Eng. Sci. *45* (1), 37-48.

BARNES, H.A., HUTTON, J.F. and WALTERS, K. 1989. Rheology of suspensions. In *An Introduction of Rheology*, pp. 115-139, Elsevier Science Pub. B.V., Netherlands.

BERNEA, E. and MIZRAHI, J. 1973. A generalized approach to the fluid dynamics of Particulate Systems. Part 1. General Correlation for fluidization and sedimentation multiparticle systems. Chem. Eng. J. *5*, 171-189.

BHAMIDIPATI, S. and SINGH, R.K. 1990. Flow behavior of tomato sauce with or without particulates in tube flow. J. Food Process Engineering *12*, 275-293.

BIRD, R.B., STEWART, W.E. and LIGHTFOOT, E.N. 1960. *Transport Phenomena*. John Wiley & Sons, Inc. New York.

BOURNE, J.R. and BUTLER, H. 1969. Power consumption of helical ribbon impellers in viscous liquids. Trans. Instn. Chem. Engrs. *47*, T263-T270.

BRITO DE LA FUENTE, E., LEULIET, J.C., CHOPLIN, L. and TANGUY, P.A. 1992. On the effect of shear thinning behavior on mixing with helical ribbon impeller. In *Process Mixing. Chemical and Biochemical Applications*. (G.B. Tatterson and R.V. Calabrese, eds.) AIChe Symp. Series *286* (88), 28-32.

CASTELL-PEREZ, M.A. and STEFFE, J.F. 1992. Using mixing to evaluate rheological properties. In *Viscoelastic Properties of Foods*, (M.A. Rao and J.F. Steffe, eds.) pp. 247-284, Elsevier Science Publishers, London.

CHAVAN, V.V. and ULBRECHT, J. 1973. Power correlations for close-clearance helical impellers in Non-Newtonian liquids. Ind. Eng. Chem. Process Des. Develop. *12* (4), 472-476.

CHAVAN, V.V. and ULBRECHT, J. 1974. Correction. Ind. Eng. Chem. Process Des. Develop. *13* (3), 309.

CROSS, M.M. and KAYE, A. 1986. Techniques for the viscometry of suspensions. Polymer Eng. Sci. *26*(2), 121–126.

DI FELICI, R., FOSCOLO, P.U., GIBILARO, L.G. and RAPAGNA, S. 1991. The interaction of particles with a fluid-particle pseudo-fluid. Chem. Eng. Sci. *46*, 1873–1877.

FRANKEL, N.A. and ACRIVOS, A. 1967. On the viscosity of a concentrated suspensions of solid spheres. Chem. Eng. Sci. *22* (6), 847–853.

GONGORA-NIETO, M.M., VERGARA-ACALL, J.L. and MARTINEZ-PADILLA, L.P. 1996. Flow behavior of food suspension model with non Newtonian continuous phase in horizontal pipe. Proceedings of 12th International Congress of Chemical and Process Engineering. Czech Society of Chemical Engineering. CHISA 96. pp. 1–10. Praha, Czech Republic.

GOVIER, G.W. and AZIZ, K. 1972. *The Flow of Complex in Pipes*, Robert E. Krieger Publishing, Florida.

HAPPEL, J. 1957. Viscosity of Suspensions of uniform spheres. J. Appl. Phys. *28* (11), 1288–1292.

JARZEBSKI, G.J. 1981. On the effective viscosity of pseudoplastic suspension. Rheol. Acta *20* (3), 281–287.

JINESCU, 1974. The rheology of suspension. Int. Chem. Eng. *14* (3), 397–420.

KEMBLOWSKY, Z. and KRISTIANSEN, B. 1986. Rheometry of fermentation liquids. Biotechnol. Bioeng. *28*, 1474–1483.

KOICHI, L., KEISHI, G. and KO, H. 1991. *Power Technology Handbook*, Marcel Dekker, New York.

METZNER, A.B. and OTTO, R.E. 1957. Agitation of Non-Newtonian fluids. AIChE J. *3* (1), 3–10.

MITSCHKA, P. 1982. Simple conversion of Brookfield R.V.T. readings into viscosity functions. Rheol. Acta *21* (2), 207–209.

MOONEY, M. 1951. The viscosity of a concentrated suspension of spherical particles. J. Colloid Sci. *11* (1), 80–85.

PORDESIMO, L.O., ZURITZ, C.A. and SHARMA, M.G. 1994a. Flow behavior of coarse solid-liquid food mixtures. J. Food Eng. *21* (4), 495–511.

PORDESIMO, L.O., ZURITZ, C.A. and SHARMA, M.G. 1994b. Mathematical representation of the flow behavior of a simulated non-Newtonian coarse food mixture. Trans. ASAE *37* (4), 1231–1234.

RAO, M.A. 1987. Predicting the flow properties of food suspensions of plant origin. Food Techn. *41* (3), 85–88.

ROUSE, H. and HOWE, J.W. 1953. *Basic Mechanic of Fluids*. pp. 181, John Wiley & Sons, New York.

SKELLAND, A.H.P. 1967. Non-Newtonian Flow and Heat Transfer, John Wiley & Sons, New York.

TATTERSON G.B. 1991. Fluid mixing and gas dispersion in agitated tanks. *Power Consumption in Viscous Creeping Flow Mixing*, pp. 59–115, McGraw Hill, New York.

ULBRECHT, J.J. and CARREAU, P. 1985. Mixing of viscous Non-Newtonian fluid. In *Mixing of Liquids by Mechanical Agitation*. (J.J. Ulbrecht and G.K. Patterson, eds.) pp. 93–137, Gordon and Breach Science Publishers, New York.